



Published in final edited form as:

J Am Chem Soc. 2010 September 22; 132(37): 13064–13071. doi:10.1021/ja105530q.

Mechanistic Study of Gold(I)-Catalyzed Intermolecular Hydroamination of Allenes

Z. Jane. Wang[†], Diego Benitez[‡], Ekaterina Tkatchouk[‡], William A. Goddard III[‡], and F. Dean Toste^{*,†}

Department of Chemistry, University of California, Berkeley, California 94720 and Materials and Process Stimulation Center, California Institute of Technology, Pasadena, California, 91125

Abstract

The intermolecular hydroamination of allenes occurs readily with hydrazide nucleophiles, in the presence of 3–12% Ph₃PAuNTf₂. Mechanistic studies have been conducted to establish the resting state of the gold catalyst, the kinetic order of the reaction, the effect of ligand electronics on the overall rate, and the reversibility of the last steps in the catalytic cycle. We have found the overall reaction to be first order in gold and allene and zero order in nucleophile. Our studies suggest that the rate-limiting transition state for the reaction does not involve the nucleophile and that the active catalyst is monomeric in gold(I). Computational studies support an “outersphere” mechanism and predicts that a two-step, no intermediate mechanism may be operative. In accord with this mechanistic proposal, the reaction can be accelerated with the use of more electron deficient phosphine ligands on the gold(I) catalyst.

Keywords

hydroamination; mechanistic studies; gold(I) catalysis; allene activation; DFT calculations

Introduction

Gold(I)-catalyzed addition of carbon, oxygen, and nitrogen based nucleophiles to allenes has emerged as a powerful synthetic transformation in recent years.¹ The stability of gold(I) complexes to air and moisture renders gold catalysis a practical and mild method for bench top synthesis.² However, the mechanism of this important class of reactions is only beginning to be explored. While multiple mechanisms for the hydroamination, hydroalkoxylation and hydroarylation of allenes have been proposed, few studies regarding the nature of the active catalyst, the rate limiting step of the reaction, and the role of allene and nucleophile in the transformation have been performed.³ Part of the challenge of performing detailed kinetic studies of gold(I) catalyzed hydroamination reactions is that many of the most active catalysts employed are generated *in situ* from gold(I) trimers or the gold chloride and the corresponding silver salt, making it difficult to determine the precise concentration of catalyst employed.⁴ In 2009, we reported the intramolecular hydroamination reaction of allenes with hydrazine nucleophiles catalyzed by an isolable

*fdtoste@berkeley.edu.

‡California Institute of Technology

†University of California

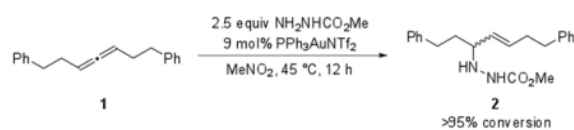
gold(I) complexes.⁵ We hypothesized that an intermolecular variant of this transformation could provide a valuable platform for a systematic study of the mechanism of the reaction.

While experimental observations in gold(III)-catalyzed hydroamination and hydroalkoxylation reactions suggest that these reactions proceed through an inner-sphere mechanism,⁶ both inner-sphere and outer-sphere mechanisms for nucleophilic addition to allenes promoted by gold(I) complexes have been proposed (Scheme 1).⁷ In the outer-sphere mechanism the cationic gold(I) complex acts as a π -acid to induce addition of the nucleophile across the C-C π -bond. Protodemetalation of the vinyl gold intermediate then regenerates the gold(I) catalyst. In the inner-sphere mechanism a tricoordinate gold complex is formed by complexation of both the allene and the nucleophile. Addition of the nucleophile across the allene then proceeds directly from this complex. In both mechanisms, a monomeric cationic gold(I) complexes are proposed to be the catalytically relevant species. However, the “aurophilicity” of gold(I)⁸ and the isolation of a vinyl-gold dimer in a gold-catalyzed hydroarylation reaction by Gagné^{3d}, suggest that dinuclear gold(I) complexes should also be considered as potential intermediates in gold(I) mediated processes. Thus, a kinetic study of this class of reactions is needed to determine the role of each reagent in the catalytic cycle and the composition of the rate limiting transition state.

Toward this goal, we have found an intermolecular gold(I)-catalyzed hydroamination reaction of allenes by hydrazide nucleophiles and investigated the mechanism of this transformation. To distinguish between the inner- and outer-sphere mechanisms, and to discover the stoichiometry of gold catalyst in the rate-determining transition state, a detailed study was performed to determine: (1) the order of the reaction in each reagent (2) the resting state of the catalyst, the nature of other intermediates within the catalytic cycle (3) the effect of electronics of the catalyst on the rate of reaction and (4) the reversibility of the reaction. These investigations provide evidence that the rate-limiting transition state involves an activated allene complex. Trapping of this complex by the nucleophile and protodemetalation to regenerate the gold catalyst are rapid and likely irreversible.

Results and Discussion

We began our studies with 1,7-diphenylhepta-3,4-diene (**1**), because the symmetry of the substrate greatly simplified the number of chemically distinct environments in which the gold(I) catalyst could coordinate. Recently, $\text{Ph}_3\text{PAuNTf}_2$ has been effectively used in the activation of carbon-carbon multiple bonds⁹ and we hypothesized that this isolable complex would be a reliable Au^+ source for mechanistic analysis. Gratifyingly, we found that **1** underwent the desired reaction with 2.5 equiv of methyl carbazate and 9 mol% $\text{Ph}_3\text{PAuNTf}_2$ in MeNO_2 at 45 °C, providing the hydroamination products in a 5:1 *trans:cis* ratio with >95% conversion after 12 h (eq 1). Monitoring the first 3.25 h of the reaction by ^1H NMR at 45 °C showed that the reaction was remarkably clean and that the total concentration of **1** and **2** during the course of the reaction was consistent with the concentration of **2** at $t = 0$ (Figure 1). In addition, the hydroamination does not proceed appreciably in the presence of 20 mol% HNTf_2 or 10 mol% AgNTf_2 . We were encouraged by these results to further examine the precise role of the $\text{Ph}_3\text{PAuNTf}_2$ in the catalytic cycle.

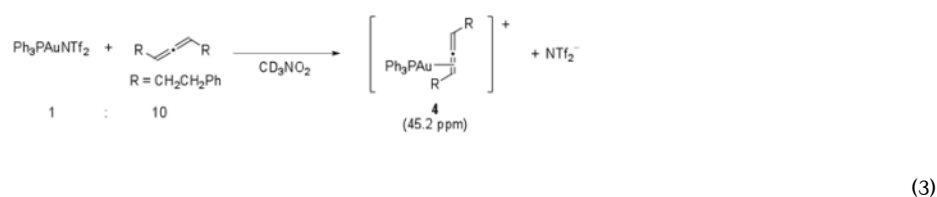
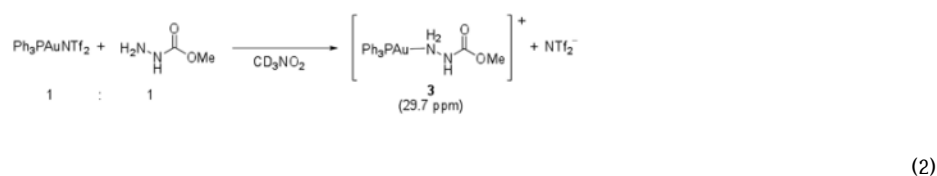


(1)

Catalyst Resting State

Phosphorous NMR methods have been previously used to study gold(I) intermediates and the ^{31}P signal of the phosphine ligand was found to be very sensitive to the electronic environment around the gold center¹⁰. Upon addition of the catalyst to a reaction mixture containing **1** and methyl carbazate, the signal corresponding to the $\text{Ph}_3\text{PAuNTf}_2$ ($\delta = 30.3$ ppm) vanished and a new signal at 45.2 ppm was observed. As the reaction progressed to higher conversion and the concentration of **1** remaining in solution was comparable to that of the catalyst, a second broad peak at 30 ppm also appeared (Figure 2).

Both gold-amine¹¹ and gold-allene¹² complexes have been previously postulated as intermediates in gold catalyzed reactions. To determine the nature of the compounds comprising the observed peaks at 30 and 45 ppm, we independently prepared two samples containing ($\text{Ph}_3\text{PAuNTf}_2$ and methyl carbazate, in a 1:1 ratio) and ($\text{Ph}_3\text{PAuNTf}_2$ and **1**, in a 1:10 ratio) in CD_3NO_2 . The sample containing $\text{Ph}_3\text{PAuNTf}_2$ and methyl carbazate showed a broadened ^{31}P NMR signal at δ 29.7 ppm (eq 2), in the same region as the second peak that appeared as catalytic reaction progressed. The second sample containing $\text{Ph}_3\text{PAuNTf}_2$ and **1**, however, showed the same ^{31}P NMR signal at 45.2 ppm as was observed in the catalytic reaction (eq 3).



The signal at 45.2 ppm is consistent with the ^{31}P NMR shifts of other alkyl- and vinyl- AuPPh_3 species reported in the literature¹³. In addition, the same species can be independently generated from a solution of Ph_3PAuCl and AgBF_4 in the presence of **1** without additional NTf_2^- . Thus, we hypothesized that this peak corresponded to a Ph_3PAu^+ -allene complex. In the catalytic reaction, this complex is in equilibrium with other cationic gold species, such as Ph_3PAu^+ and Ph_3PAu^+ -carbazate. When the concentration of **1** was relatively high at the beginning of the reaction, the equilibrium favored the gold-allene complex. As the reaction progressed, the concentration of **1** decreased and the equilibrium shifted such that the other cationic gold species were also observable by NMR.¹⁴

Due to the C_2 symmetry of the allene, two diastereotopic π -gold complexes could theoretically be formed; yet we could not resolve the two complexes by either ^{31}P or ^1H NMR at low temperature (0 to -84 °C). However, computational studies have predicted the barrier for exchange between the two diastereomeric faces of a simple disubstituted alkyl allene to be very low¹⁵. In addition, the energy difference between the two π -complexes that could form is calculated to be only 1.0 kcal/mol. Thus, it is likely that under catalytic reaction conditions, this species is two-coordinate cationic gold-allene complex with a fully

dissociated counterion, where the gold center is rapidly exchanging between the two faces of the allene.

Kinetic Order of the Reaction

Order in Nucleophile—In order to determine the rate-determining transition state for the catalytic reaction, we sought to establish kinetic order of the reaction in $\text{Ph}_3\text{PAuNTf}_2$, **1**, and methyl carbazate. We began our studies by examining the order of the $\text{Ph}_3\text{PAuNTf}_2$ catalyzed hydroamination reaction in nucleophile by the method of initial rates. The allene (**1**) (90.9 mM) and $\text{Ph}_3\text{PAuNTf}_2$ (5.45 mM) was combined with varying concentrations of methyl carbazate from 90.0 to 295.5 mM in CD_3NO_2 at 45 °C. The reactions were monitored by ^1H NMR and a plot of k_{obs} ,¹⁶ (as determined by $(\Delta[\mathbf{2}]/\Delta t)/[\mathbf{1}]_0$, where $[\mathbf{1}]_0 = 90.91$ mM) at each concentration of methyl carbazate provided a straight line with $R^2 = 0.9923$ and a slope of -0.0001 h^{-1} (Figure 3). The order in methyl carbazate was verified by a least squares fit to $f(x) = ax^n$, which provided $n = -0.108$ (Supporting Information, Figure S3). These results indicate that methyl carbazate is not involved in the rate-determining transition state. In contrast, previously proposed mechanisms have implied nucleophilic addition or protodemetalation to be the rate-limiting step in gold(I) catalyzed hydroamination¹⁷.

Order in Allene—The order in **1** was next determined by monitoring the reaction of **1** (150 mM), methyl carbazate (325 mM) and $\text{Ph}_3\text{PAuNTf}_2$ (13.5 mM) in CD_3NO_2 at 45 °C (Figure 4) by ^1H NMR.¹⁸ The reaction followed pseudo first order kinetics in **1** and provided linear plots of $-\ln([\mathbf{1}]_t/[\mathbf{1}]_0)$ vs. time with $R^2 = 0.9995$. The pseudo first order rate constants (k_{obs}) measured reflects the rate of formation of both trans and cis hydroamination products. The first order dependence on **1** implies that the allene is involved in the turnover limiting transition state and that there is an equilibrium between the free and gold-bound allene.

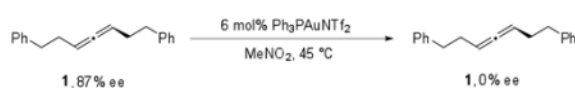
Order in Gold—The order in $\text{Ph}_3\text{PAuNTf}_2$ was examined by measuring the pseudo-first order rate constant, k_{obs} , for the reaction at various catalyst loadings. Allene **1** (150 mM) and methyl carbazate (325 mM) were combined with various concentrations of $\text{Ph}_3\text{PAuNTf}_2$ (4.5 to 18 mM) in CD_3NO_2 at 45 °C. Plotting the measured k_{obs} of the reaction at a range of catalyst loadings provided a straight line with $R^2 = 0.9993$ (Figure 5). This result suggests that the overall reaction is first order in gold and implies that the rate-limiting transition state contains only one gold center.

Hammett Analysis: Our group has previously investigated the ability ligand electronics to affect the rate of certain pathways in a gold(I) catalyzed process.¹⁹ Thus, a Hammett study of the reaction was performed to probe the sensitivity of the reaction to changes in the electronic properties of the phosphine ligand in the $\text{Ar}_3\text{PAuNTf}_2$ catalyst. Toward this goal, phosphine gold catalysts bearing substitution in the *para* position were prepared. The reaction of **1** (150 mM) and methyl carbazate (325 mM) in the presence of 6 mol % (*p*-X- C_6H_4) $_3\text{PAuNTf}_2$ (X = CF_3 , Cl, H, and OMe) in CD_3NO_2 at 45 °C was monitored by ^1H NMR. Plotting $\log[(k_{\text{obs,X}})/(k_{\text{obs,H}})]$ against σ provided a straight line ($R^2 = 0.96$) with $\rho = 0.21$ (Figure 6). A positive ρ value is consistent with a decrease in partial positive charge on the phosphine ligand in the transition state. The kinetic order and Hammett analysis of the reaction are consistent with the gold(I) activation of allene as the rate-limiting transition state in the catalytic cycle.

Chirality Transfer: We sought to determine whether chirality transfer was possible from the allene to the hydroamination product to determine whether the reaction went through chiral or planar gold intermediates. While trisubstituted allenes are known to racemize rapidly in the presence of gold(I) catalysts,²⁰ good chirality transfer has been observed with

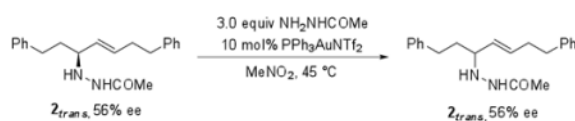
some unfunctionalized disubstituted allenes.²¹ In addition, chirality transfer would exclude a planar allyl cation as part of the catalytic cycle, as such a species would lead to complete racemization. Enantioenriched **1** (101 nM, 87% ee) was prepared by the method described by Myers²² and was combined with methyl carbazate and Ph₃PAuNTf₂ at 45 °C. The enantiomeric excess of the major hydroamination product **2_{trans}** was determined by chiral HPLC analysis and summarized in Table 1.

Interestingly, though some chirality transfer was observed at all concentrations of nucleophile, the highest levels of transfer were observed for reactions where greater than 4 equiv of methyl carbazate was used. This indicates that the reaction cannot be proceeding exclusively through a planar intermediate. In addition, the ability of nucleophile concentration to affect chirality transfer suggests that racemization can occur from the chiral allyl-gold intermediate and this process proceeds at a rate competitive with trapping of the intermediate by methyl carbazate. In the absence of any nucleophile, **1** completely racemizes in the presence of the catalyst after 12 h at 45 °C (eq 4).



(4)

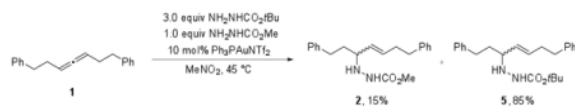
Reversibility of the Reaction: While protodeauration of the gold catalyst is conventionally depicted as an irreversible process in a catalytic reaction, Lee recently reported an example of reversible hydroalkoxylation²³ in the presence of Ph₃PAuNTf₂. Furthermore, an irreversible reaction under catalytic conditions would allow us to exclude the possibility that the incomplete chirality transfer we observed previously was due to racemization of the product. To probe whether the intermolecular hydroamination reaction is reversible, enantioenriched **2** (56% ee) was subjected to 2 equiv of methyl carbazate and 10 mol % achiral Ph₃PAuNTf₂. After 6 h at 45 °C, **2** was recovered in 56% ee with no apparent erosion of enantiopurity (eq 9), supporting an irreversible protodemetalation. However, conservation of enantiomeric excess could also result from a reversible reaction that regenerates an enantioenriched allene-gold intermediate that can then reform **2** with good chirality transfer.



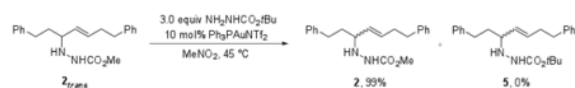
(5)

We hypothesized that a competition experiment with a second hydrazide nucleophile would be able to distinguish between these possibilities. If a chiral allene or gold-allene complex was indeed being reversibly formed, hydroamination products from trapping with both hydrazide nucleophiles should be observed. In a competition experiment with 1 equiv methyl carbazate and 3 equiv *t*-butyl carbazate, both hydroamination products were observed in a 15:85 ratio in >95% conversion, indicating that formation of **5** is kinetically competitive with formation of **2**. Thus, if the reaction is reversible and **2** is resubjected to catalytic conditions in the presence of 3 equiv of *t*-butyl carbazate, a mixture of **2** and **5** should be expected. However, heating the reaction to 45 °C for 8 hr produced **2** as the sole

product. The lack of detectable amounts of **5** indicated that chiral allene or gold-allene intermediates could not be forming reversibly under the reaction conditions.



(6)



(7)

Mechanistic Discussions

To corroborate the kinetic data observed and to gain insight into the nature of the intermediates in the catalytic cycle, we investigated the mechanism for hydroamination of allenes using density functional theory (DFT) with the B3LYP and M06 functionals. We used the experimental observations as a guide for exploring the geometry and potential energy surface for the reaction. We investigated the catalytic reaction of model (*S*)-penta-2,3-diene, methyl carbazate and $\text{Ph}_3\text{PAu(I)}^+$. We calculated the free energy of coordination of the allene to $\text{Ph}_3\text{PAu(I)}^+$ to be -9.2 kcal/mol, in favor of the allene-gold complex **A**.²⁴ Activation of **A** proceeds through transition state **TS1**, which lies 4.9 kcal/mol higher in energy than the planar, cationic gold(I) complex **6**. Though the methyl carbazate is included in calculations, the nucleophile itself is not associated with **TS1** or **6**. Malacria and co-workers reported¹⁵ that the steric hindrance at the allylic positions determines the energies and stabilities of the possible isomeric forms of the planar, cationic gold(I) complex. In agreement with their analysis, we find that only intermediate **6** is stable. In comparison, intermediates **7** and **8** are not minima and relax to **A** or **A'**.

As we moved further along the reaction coordinate, a second transition state (**TS2**) involving the addition of methyl carbazate to allene-gold specie was found. We find that transition state **TS1** leads to adjacent transition state **TS2** without an intervening intermediate. On the basis of our experimental observations and calculations, we propose a *two-step, no intermediate*²⁵ process similar to the one described by Nevado for a Au(I) catalyzed cyclization.²⁶ The geometry of the allene fragment in **TS1** and **TS2** resemble a bent allene geometry.¹⁵ Intermediate **B** ($\Delta G = -14.8$ kcal/mol) undergoes protodeauration leading to product ($\Delta G = -24.1$ kcal/mol), in agreement with the irreversibility of the reaction.

The absence or presence of a short-lived intermediate between transition states **TS1** and **TS2** is affected by the relative concentration and reactivity of the nucleophile, and thus relates directly to the magnitude of chirality transfer. The reaction coordinate bifurcates following **TS1**, leading to **TS2** or intermediate **6**. At higher nucleophile concentrations, addition of the nucleophile is fast and the *two-step no intermediate* pathway is favored, leading to higher levels of chirality transfer. At lower concentrations of nucleophile, **TS1** leads to the planar intermediate **6** with loss of chirality. The operating reaction mechanism is a continuum between a traditional *two-step* process with loss of chirality and a *two-step no-intermediate* process with retention of the stereochemistry.

We studied the structural and electronic details of the located transition structures and compared them to Au-allene coordinated complex **A**. Shown in Figure 7 are key metrical parameters and natural charges derived from natural population analyses of the corresponding M06 wave function. We find that for **A**, the charge on C³ is least negative (vs. C¹), while the charge on C¹ is most negative of the allene carbon atoms.

On the basis of the kinetic, ligand effect, reversibility, chirality transfer, and computational studies performed, we propose a mechanistic picture for the gold(I)-catalyzed hydroamination of allenes, as shown in Scheme 4. The resting state of the catalyst is consistent with a cationic gold-allene complex that is rapidly exchanging between the two diastereomeric faces of the C₂ symmetric allene and is in equilibrium with other cationic gold species, denoted [Au⁺]. Our computational studies suggest that a bent allene-gold complex is the rate determining transition state (**TS1**) in the catalytic cycle and our kinetic data provides direct experimental support for these calculations. The overall reaction exhibits zeroth order dependence on the concentration of nucleophile, suggesting that nucleophilic addition must occur after the rate-determining step. This observation is in agreement with calculated free energy of **TS2**, which is 3.6 kcal/mol lower than that of **TS1**. In addition, the pseudo first order dependence on the concentration of allene and Ph₃PAuNTf₂ suggest that the catalytic species is monomeric and that the ratio of allene to catalyst in the transition state is 1:1. Thus, an innersphere mechanism where the nucleophile coordinates to the gold center prior to or during allene activation is unlikely, as such a mechanism would exhibit positive order in nucleophile.

We have demonstrated that the nucleophilic addition and protodemetalation steps are irreversible under catalytic conditions and occur after the rate limiting transition state. Thus, our reaction can be simplified and modeled using Michaelis-Menten kinetics. The general rate law of the reaction follows the Michaelis-Menten equation (eq 8). The K_M for the reaction can be calculated from a Line weaver-Burke plot of our kinetic data and was found to be 3.9(1.5)×10³ mM (Supporting Information, Figure S8). Thus under the conditions examined, the concentration of **1** is small relative to ₂₇ K_M and the Michaelis-Menten equation can be reduced to eq 9, providing a rate law that is first order in gold and **1**.

$$\text{rate} = \frac{k_2[\text{Ph}_3\text{PAuNTf}_2][\mathbf{1}]}{[\text{S}] + K_M} \quad \text{where } K_M = \frac{k_2 + k_{-1}}{k_1} \quad (8)$$

$$\text{rate} = \frac{k_2[\text{Ph}_3\text{PAuNTf}_2][\mathbf{1}]}{K_M} = k_{\text{obs}}[\text{Ph}_3\text{PAuNTf}_2][\mathbf{1}] \quad \text{where } k_{\text{obs}} = \frac{k_2 k_1}{k_2 + k_{-1}} \quad (9)$$

A Hammett study of the reaction demonstrates that changing the electronics of the Ar₃P ligand noticeably affected the rate of reaction and provides quantitative evidence that gold(I) reactivity can be modulated by ligand electronics. In particular, phosphines with electron-withdrawing *para* substituents increased the rate of the reaction while electron-donating substituents slow the reaction relative to Ph₃PAuNTf₂. This is consistent with a rate-determining transition state that exhibits a reduction in δ⁺ character on the phosphine relative to the ground state. Our proposed transition state allows for the delocalization of positive charge from the Ph₃PAu⁺ onto the allenic fragment, and is hence consistent with the ρ value observed. Furthermore, the inability to regenerate the gold-allene intermediate from the isolated hydroamination products (**2**) under catalytic conditions suggests that either one or both the addition or the protodemetalation steps are irreversible.

Conclusions

We have reported the first example of intermolecular hydroamination of allenes with a N-N linked nucleophile in the presence of a gold(I) catalyst, $\text{Ph}_3\text{PAuNTf}_2$. This system has allowed us to conduct the first detailed kinetic study of the mechanism of gold(I)-mediated allene activation. Our experiments provide experimental evidence that allene activation is the rate-limiting step in gold(I)-catalyzed addition of hydrazide nucleophiles to allenes. Computational studies show that the reaction examined proceeds via a two-step no-intermediate mechanism and that the second transition state immediately following the rate determining step is not planar, but likely axially chiral. Importantly, the dependence of the degree of chirality transfer on the concentration of the nucleophile suggests that a pathway proceeding through a traditional two-step pathway involving a planar intermediate is also available. This mechanistic study has important implications for the future development of racemic and enantioselective C-X bond forming reactions *via* addition of a nucleophiles to allenes promoted by gold(I). Using these mechanistic insights, we are currently working toward developing and investigating the mechanism of gold(I)-catalyzed additions of various nucleophiles to allenes.

Supplementary Material

Refer to Web version on PubMed Central for supplementary material.

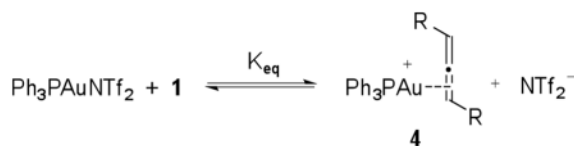
Acknowledgments

We thank the NIHGMS (R01 GM073932) and the Director, Office of Science of the U.S. Department of Energy under Contract No. DE-AC02-05CH11231 for funding and Johnson Matthey for a generous donation of AuCl_3 . Z. J. Wang thanks the Hertz Foundation for a graduate fellowship. We are also grateful to Dr. Robert Bergman for support during the kinetic studies. Computational facilities were funded by grants from ARO-DURIP and ONR-DURIP.

References

1. For general reviews, see: (a) Gorin DJ, Sherry BD, Toste FD. *Chem Rev.* 2008; 108:3351. [PubMed: 18652511] (b) Jiménez-Núñez E, Echavarren AM. *Chem Commun.* 2007:333. (c) Furstner A, Davies PW. *Angew Chem, Int Ed.* 2007; 46:3410. (d) Hashmi ASK. *Chem Rev.* 2007; 107:3180. [PubMed: 17580975] (e) Shen HC. *Tetrahedron.* 2008; 64:3885. (f) Li Z, Brouwer C, He C. *Chem Rev.* 2008; 108:3239. [PubMed: 18613729]
2. (a) Gorin DJ, Toste FD. *Nature.* 2007; 446:395. [PubMed: 17377576] (b) Shapiro ND, Toste FD. *Synlett.* 2010:675. [PubMed: 21135915]
3. For examples, see: (a) Zhang Z, Liu Cong, Kinder RE, Han X, Qian H, Widenhoefer RA. *J Am Chem Soc.* 2006; 128:9066. [PubMed: 16834380] (b) Nishina N, Yamamoto Y. *Tetrahedron.* 2009; 65:1799. (c) Duncan AN, Widenhoefer RA. *Synlett.* 2010:419. [PubMed: 21197142] (d) Weber D, Tarselli MA, Gagné MR. *Angew Chem Int Ed.* 2009; 48:5733.
4. For selected examples, see: (a) Hyland CT, Hegedus LS. *J Org Chem.* 2006; 71:8658. [PubMed: 17064053] (b) Zhang Z, Bender CF, Widenhoefer RA. *J Am Chem Soc.* 2007; 129:14148. [PubMed: 17967025] (c) Liu C, Widenhoefer RA. *Org Lett.* 2007; 9:1935. [PubMed: 17428061] (d) Piera J, Krumlinde P, Strübing D, Bäckvall JE. *Org Lett.* 2007; 9:2235. [PubMed: 17465562] (e) Hamilton GL, Kang EJ, Mba M, Toste FD. *Science.* 2007; 317:496. [PubMed: 17656720] For an example of a gold(I) trimer precatalyst, see: (f) Sherry BD, Maus L, Laforteza BN, Toste FD. *J Am Chem Soc.* 2006; 128:8132. [PubMed: 16787066]
5. Lalonde RL, Wang JZ, Mba M, Lackner AD, Toste FD. *Angew Chem Int Ed.* 2009; 49:598.
6. Nishina N, Yamamoto Y. *Angew Chem Int Ed.* 2006; 45:3144.
7. For proposed outersphere mechanisms, see: (a) Widenhoefer RA, Han Q. *Eur J Org Chem.* 2006:4555. and Reference 3a. For proposed innersphere mechanisms, see: (b) Zeng X, Soleilhavoup M, Bertrand G. *Org Lett.* 2009; 11:3166. [PubMed: 19719176] and reference 3b. For evidence of

- gold-catalyzed outersphere hydroamination of alkenes, see: (c) LaLonde RL, Brenzovich WE Jr, Benitez D, Tkatchouk E, Kelley K, Goddard WA III, Toste FD. *Chem Sci*. 2010; 1:226.
8. (a) Schmidbaur H. *Gold Bulletin*. 2000; 33:3. (b) Scherbaum F, Grohmann A, Huber Brigitte, Kruger C, Schmidbaur H. *Angew Chem Int Ed*. 1988; 27:1544. (c) Cheong PH, Morganelli P, Luzung MR, Houk KN, Toste FD. *J Am Chem Soc*. 2008; 130:4517. [PubMed: 18327944]
9. (a) Mezailles N, Ricard L, Gagosz F. *Org Lett*. 2005; 7:4133. [PubMed: 16146370] (b) Toullec PY, Blarre T, Michelet V. *Org Lett*. 2009; 11:2888. [PubMed: 19480435]
10. (a) Grisé CM, Barriault L. *Org Lett*. 2006; 8:5905. [PubMed: 17134302] (b) Grisé CM, Rodrigue EM, Barriault L. *Tetrahedron*. 2008; 64:797. (c) Seidel G, Mynott R, Fürstner A. *Angew Chem Int Ed*. 2009; 48:2510.
11. Mizushima E, Hayashi T, Tanaka M. *Org Lett*. 2003; 5:3349. [PubMed: 12943424] Also see reference 3b and 7b.
12. (a) Mauleon P, Krinsky JL, Toste FD. *J Am Chem Soc*. 2009; 131:4513. [PubMed: 19275228] (b) Benitez D, Tkatchouk E, Gonzales AZ, Goddard WA III, Toste FD. *Org Lett*. 2009; 11:4798. [PubMed: 19780543] (c) Deutsch C, Gockel B, Hoffman-Roder A, Krause N. *Synlett*. 2007; 11:1790. For an example with gold(III), see: Morita N, Krause N. *Org Lett*. 2004; 6:4121. [PubMed: 15496114]
13. (a) Hashmi ASK, Ramamurthi TD, Rominger F. *J Organomet Chem*. 2009; 694:592. (b) Shi Y, Ramgren SD, Blum SA. *Organometallics*. 2009; 28:1275. (c) Mohr F, Falvello LR, Laguna M. *Eur J Inorg Chem*. 2006:833. (d) Porter KA, Schier A, Schmidbaur H. *Organometallics*. 2003; 22:4922. (e) Herrero-Gómez E, Nieto-Oberhuber C, López J, Benet-Buchholz J, Echavarran AM. *Angew Chem Int Ed*. 2006; 45:5455.
14. The composition of the cationic gold species observed under catalytic conditions could not be determined as both Ph_3PAu^+ and **3** show phosphorous NMR signals around 30 ppm. However, in the absence of nucleophile, the K_{eq} for the equilibrium between **1**, $\text{Ph}_3\text{PAuNTf}_2$, and **4** was found to be 1.32 at 50 °C using ^{31}P NMR techniques with PPh_3 internal standard.



- This value is within an order of magnitude to the K_{eq} reported for structurally similar gold(I) π -alkene complexes. For example, see Brown TJ, Dickens MG, Widenhofer RA. *J Am Chem Soc*. 2009; 131:6350. [PubMed: 19368391]
15. Gandon V, Lemi re G, Hours A, Fensterbank L, Malacria M. *Angew Chem Int Ed*. 2008; 47:7534.
16. The pseudo first order rate constants (k_{obs}) measured reflects the rate of formation of both *trans* and *cis* hydroamination products.
17. For examples involving showing nucleophilic addition as the first irreversible step in the catalytic cycle, see ref. 3b and (a) Kinder RE, Zhang Z, Widenhofer RA. *Org Lett*. 2008; 10:3157. [PubMed: 18570376] For studies involving hydroamination of dienes and olefins, see (b) Kovacs G, Ujaque G, Lledos A. *J Am Chem Soc*. 2008; 130:853. [PubMed: 18166047] and ref 7c.
18. Also see Supporting Information, Figure S4.
19. Mauleon P, Zeldin RM, Gonzalez AZ, Toste FD. *J Am Chem Soc*. 2009; 131:6348. [PubMed: 19378998]
20. (a) Sherry BD, Toste FD. *J Am Chem Soc*. 2004; 126:15978. [PubMed: 15584728] (b) Lee JH, Toste FD. *Angew Chem Int Ed*. 2007; 46:912.

21. (a) Zhang Z, Widenhoefer RA. *Org Lett.* 2008; 10:2079. [PubMed: 18412355] (b) Patil NT, Lutete LM, Nishina N, Yamamoto Y. *Tetrahedron Lett.* 2006; 47:4749.
22. Myers AG, Zheng B. *J Am Chem Soc.* 1996; 118:4492.
23. Hadfield MS, Lee A. *Org Lett.* 2010; 12:484. [PubMed: 20050603]
24. We calculate isomer A' to be ~1 kcal/mol higher in free energy than A.
25. Singleton DA, Hang C, Szymanski MJ, Meyer MP, Leach AG, Kuwata KT, Chen JS, Greer A, Foote CS, Houk KN. *J Am Chem Soc.* 2003; 125:1319. [PubMed: 12553834]
26. Garayalde D, Gomez-Bengoa E, Huang XG, Goeke A, Nevado C. *J Am Chem Soc.* 2010; 132:4720. [PubMed: 20225807]
27. The concentration of substrate examined in our kinetic experiments ranged from 90.1 mM to 150 mM.

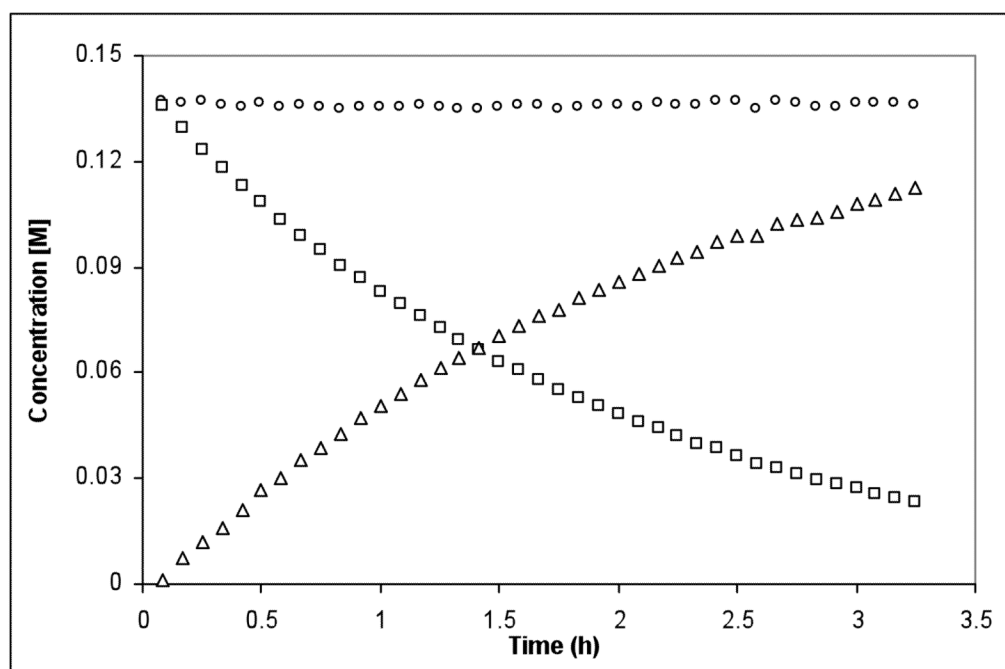


Figure 1. Reaction of **1** with methyl carbazate where $\square = [1]$, $\Delta = [2]$, and $\circ = [1] + [2]$.

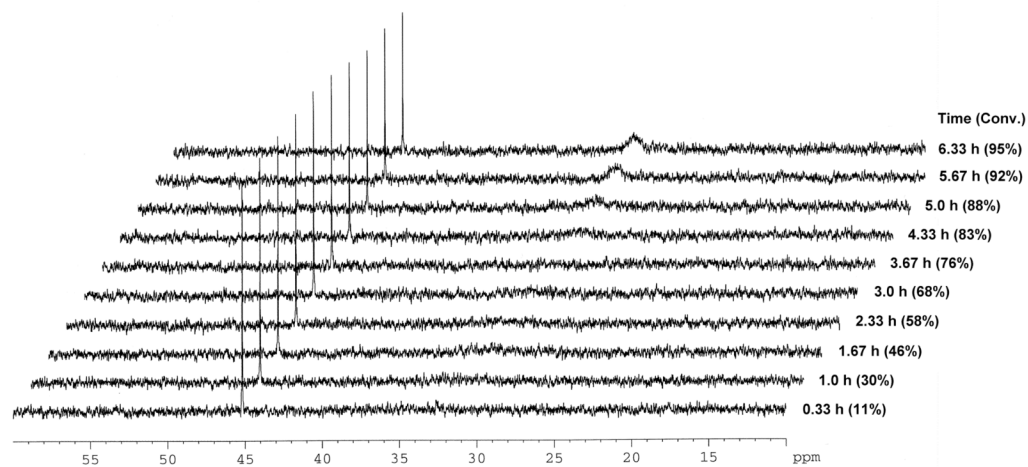


Figure 2.
The hydroamination reaction was monitored by ^{31}P NMR spectroscopy.

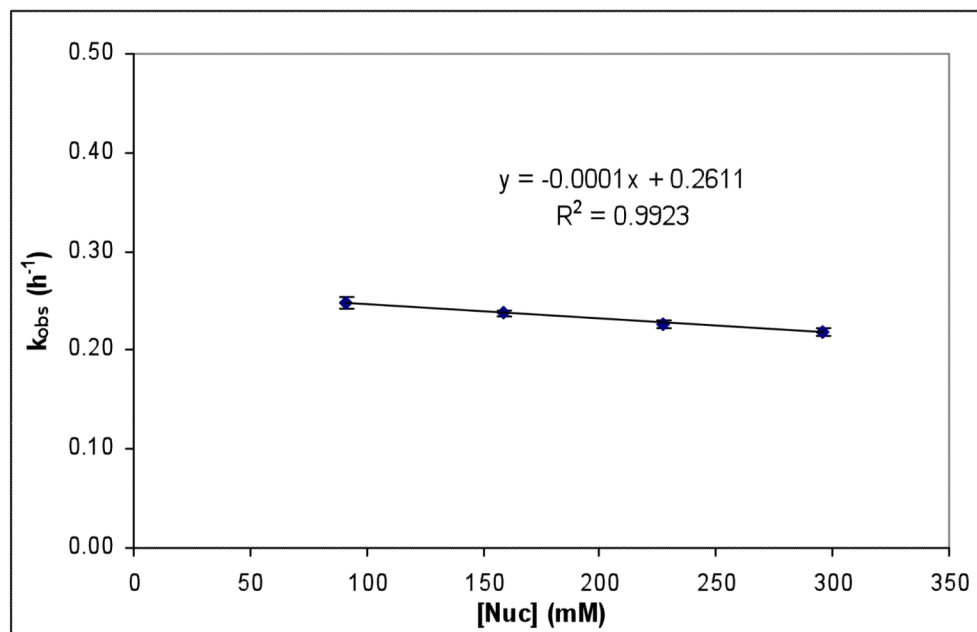
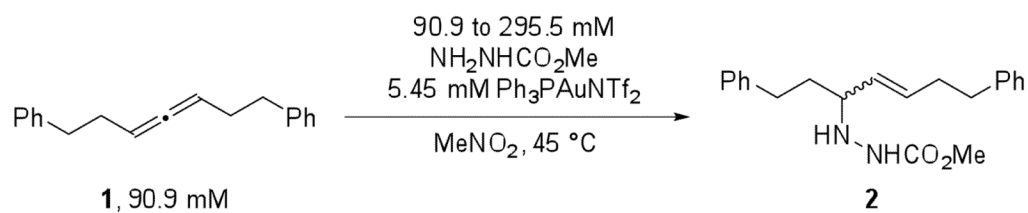


Figure 3.

A plot of k_{obs} versus concentration of methyl carbamate, where k_{obs} was determined by the method of initial rates.

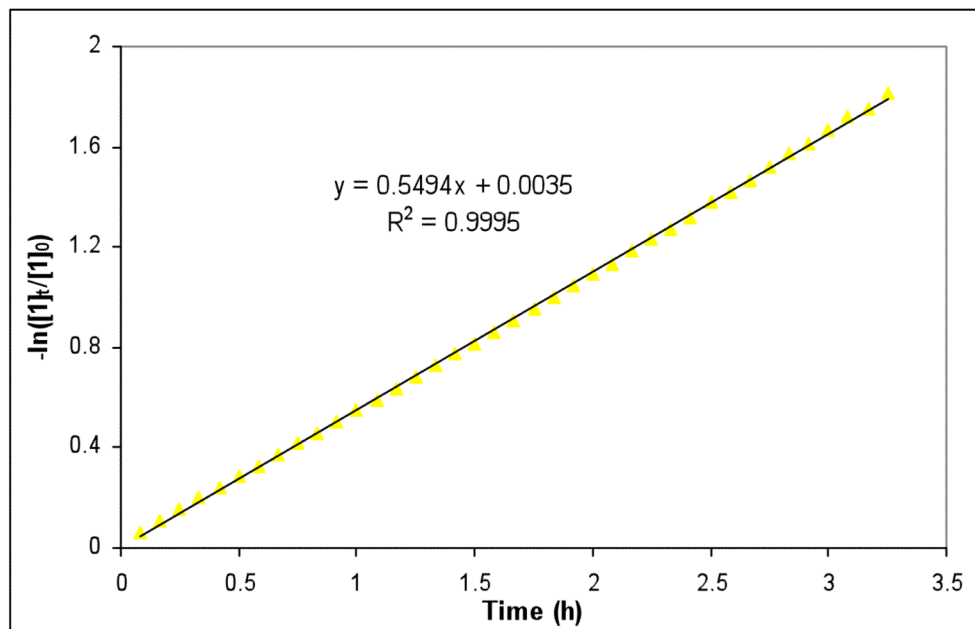
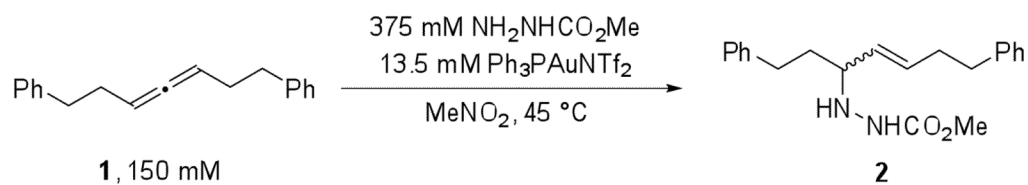


Figure 4. A representative plot of $-\ln[1(t)/1_0]$ versus time (h) for the reaction of **1** and methyl carbazate shows first order dependence in **1**.

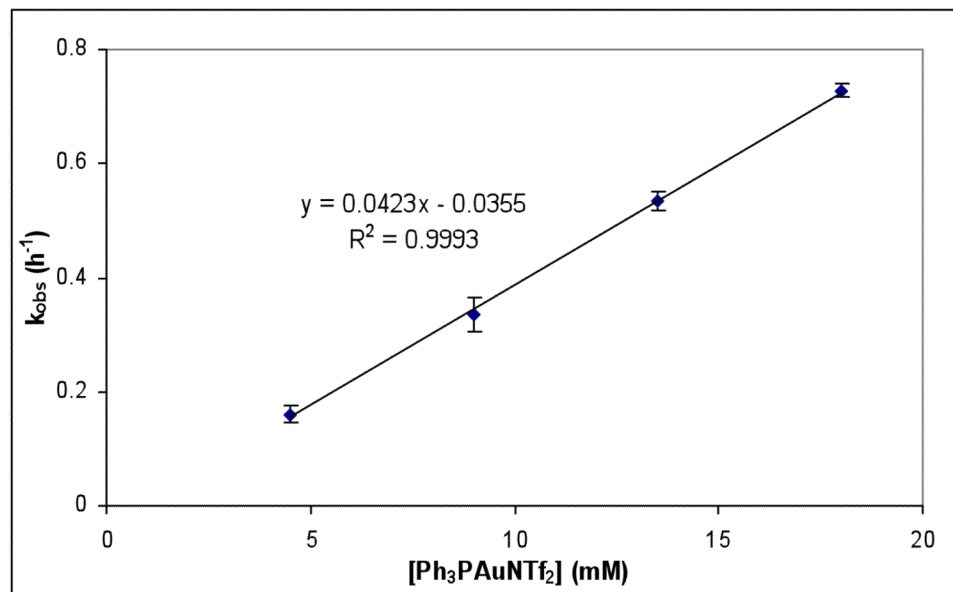
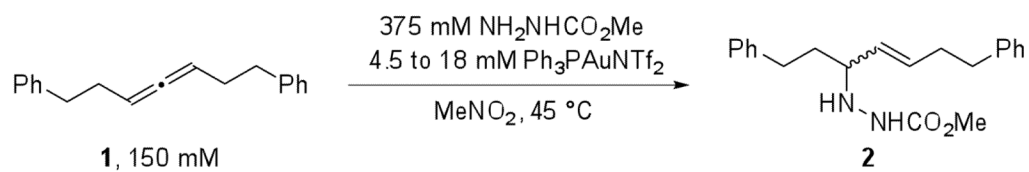


Figure 5. A plot of k_{obs} versus $[\text{Ph}_3\text{PAuNTf}_2]$, using 2.5 equiv methyl carbazate.

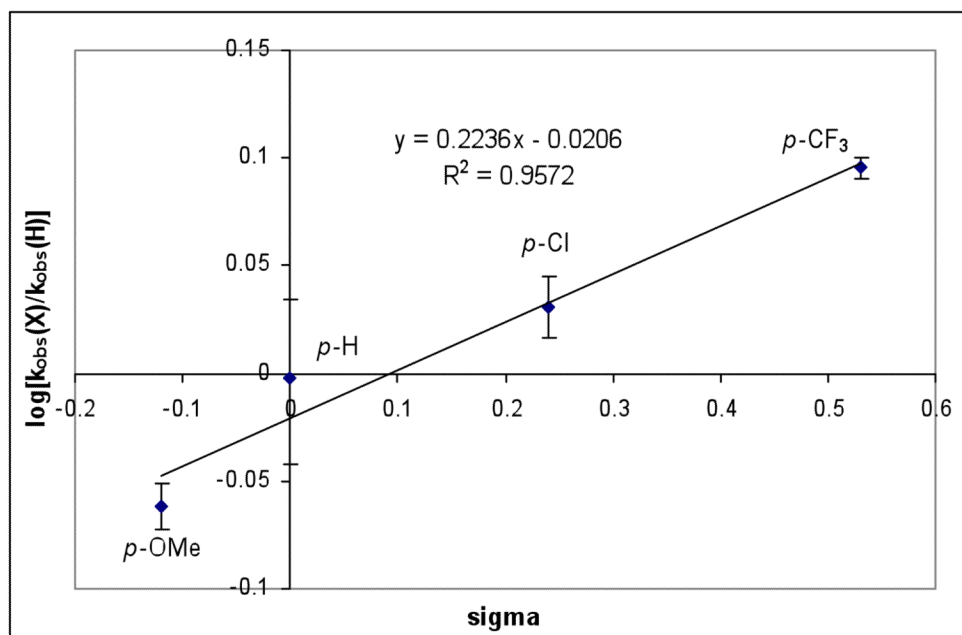
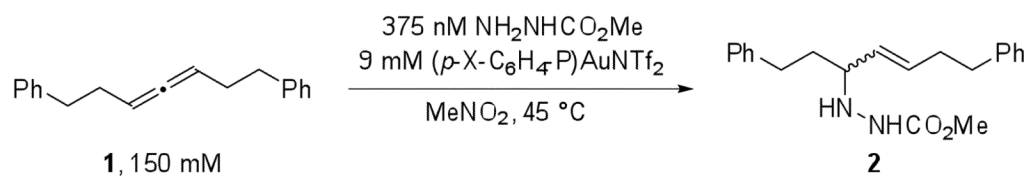


Figure 6. A Hammett plot of k_{obs} for hydroamination of **1** in the presence of $\text{Ar}_3\text{PAuNTf}_2$.

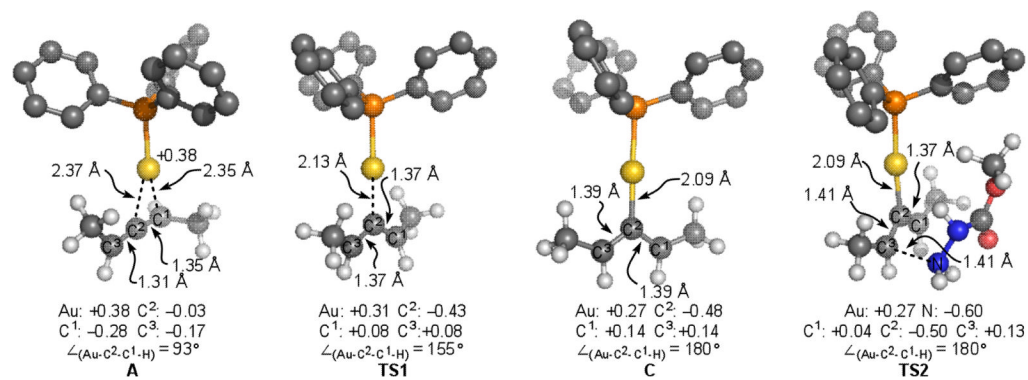
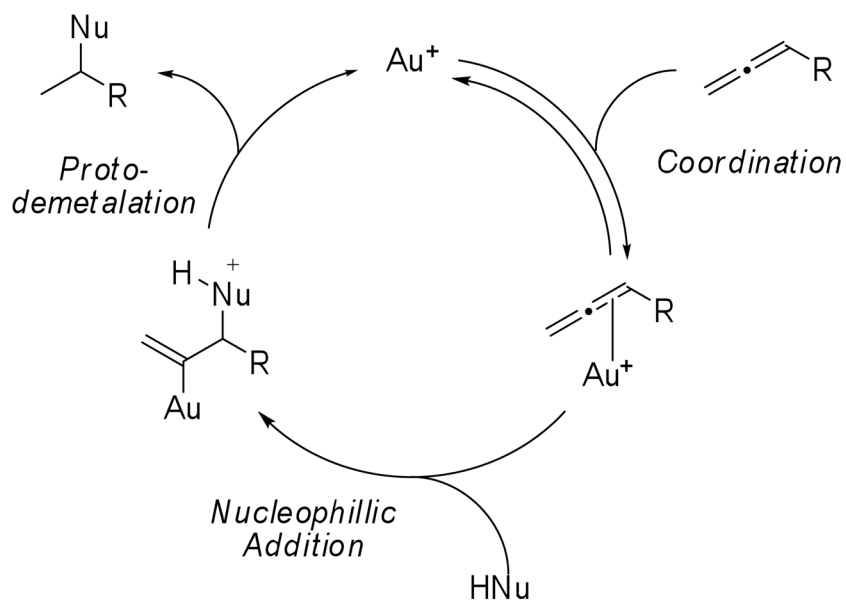
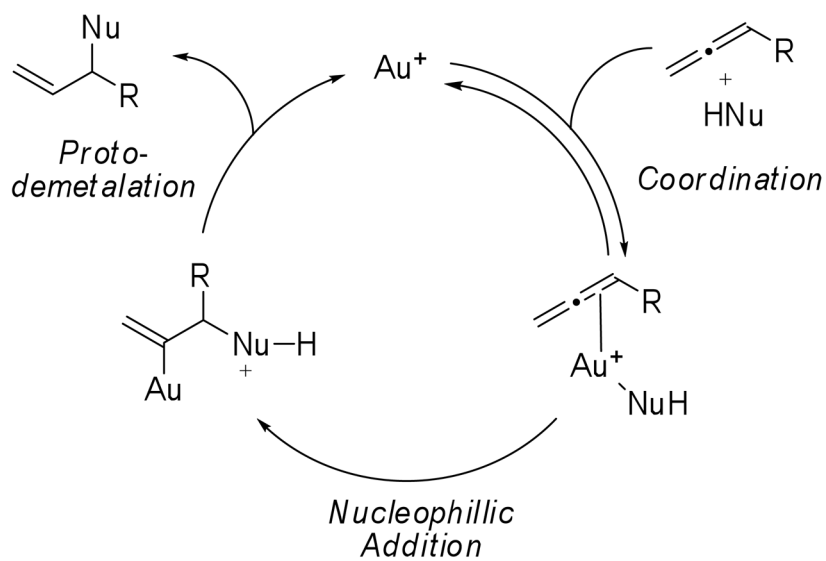
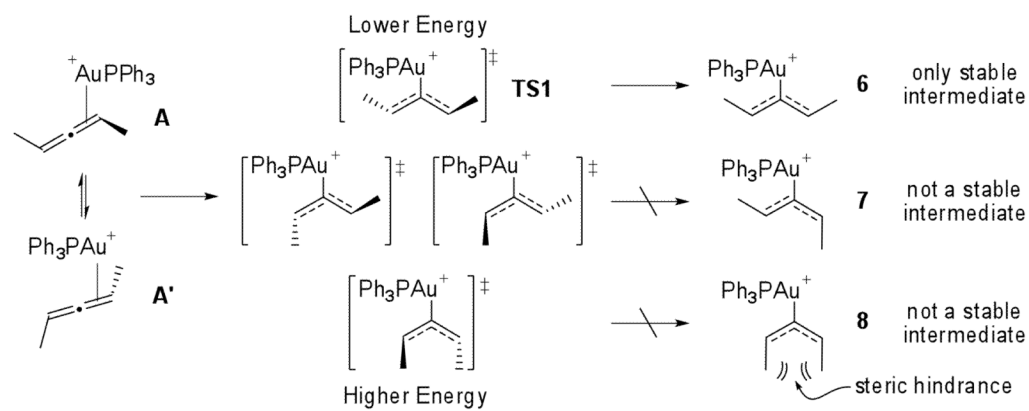


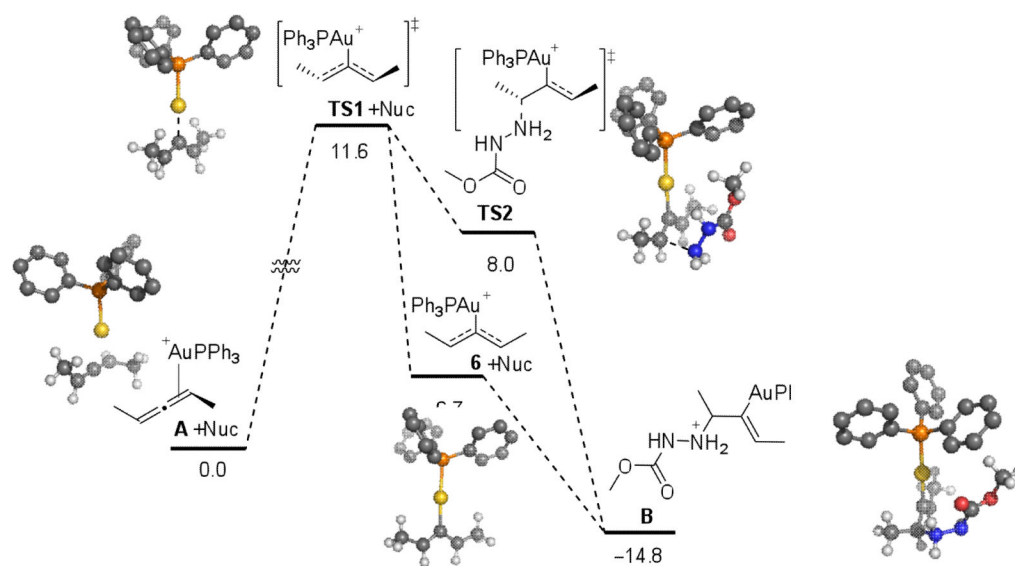
Figure 7.
Structural and natural atomic charge of selected complexes.

Outersphere Pathway**Innersphere Pathway****Scheme 1.**

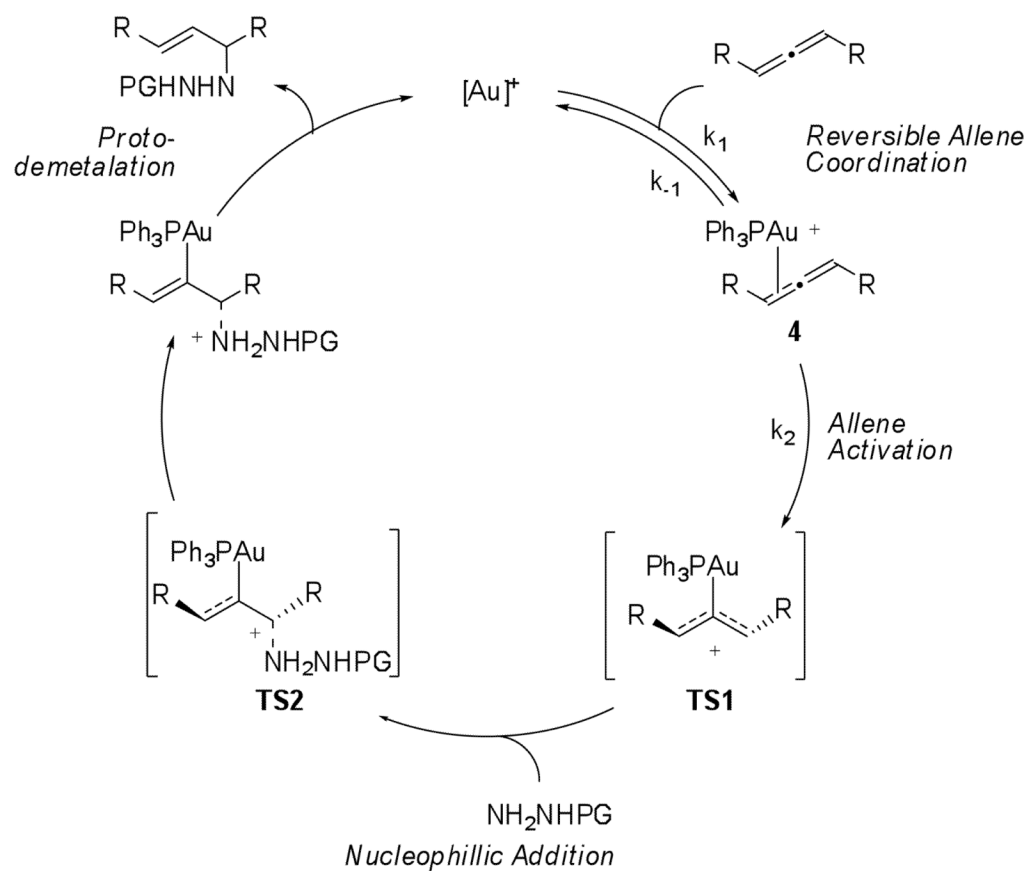
Outersphere and innersphere mechanisms proposed for the hydroamination of allenes with gold(I) catalysts.

**Scheme 2.**

Geometries of (*S*)-penta-2,3-diene and [Ph₃PAu]⁺ as coordination, transition state, and allylic cation complexes.

**Scheme 3.**

Partial reaction coordinate diagram for Au(I) catalyzed hydroamination of (*S*)-penta-2,3-diene. Energy values are free energies (ΔG) for the lowest energy isomer at 298 K.

**Scheme 4.**

Proposed mechanism for hydroamination of **1** with $Ph_3PAuNTf_2$.

Table 1

Chirality transfer for the hydroamination of chiral **1** in the presence of $\text{Ph}_3\text{PAuNTf}_2$ catalyst at various equiv of methyl carbazate.

